Accurate Characterization of an Inductive Strip in Finline

ANIMESH BISWAS, STUDENT MEMBER, IEEE, AND BHARATHI BHAT, SENIOR MEMBER, IEEE

Abstract —**The problem of an inductive strip in a finline cavity is solved by applying the transverse resonance technique. The choice of accurate basis functions for the slot field distributions has made possible an accurate determination of inductive strip discontinuity parameters. The computed results are shown to match well with the experiments and also with the experimental data available in the literature.**

I. Introduction

THE CHARACTERIZATION of finline discontinuities has been a subject of considerable research interest in recent years [1]–[5]. This is because an accurate knowledge of the discontinuity parameters allows more accurate design of practical finline circuits. Of the various types of discontinuities encountered in practice, the inductive strip is an important one, especially for the realization of the resonator elements and multiresonator filter circuits. This type of discontinuity has been analyzed by using an approximate equivalent rectangular waveguide model by Saad and Schunemann [1] and by applying the rigorous hybrid-mode spectral-domain approach developed by Koster and Jansen [2]. Recently, Knorr and Deal [3] have reported both theoretical and experimental results of the scattering coefficients of an inductive strip in finline. Their theoretical results are based on a spectral-domain analysis of the finline cavity housing the strip discontinuity.

While the spectral-domain technique is rigorous, the accuracy of the numerical results of the discontinuity parameters depends to a large extent on the accuracy of the choice of basis functions for the slot field distribution. In this paper, we use the transverse resonance method [5] to analyze the theoretical model of a finline cavity housing an inductive strip. More importantly, accurate basis functions have been chosen for the slot field distributions, which have allowed a more accurate evaluation of strip discontinuity parameters.

II. Theoretical Analysis

Consider the model of a unilateral finline cavity with an inductive strip discontinuity placed symmetrically with respect to the two ends of the cavity. The cross-sectional view of the unilateral finline and the conductive pattern on the substrate are shown in Fig. 1.

In view of the symmetry of the structure with respect to the plane PP', it is sufficient to analyze one half of the structure by placing an electric wall at PP' for the odd-mode excitation and a magnetic wall at PP' for the even-mode excitation. The expressions for the x component of the electric and magnetic fields in the three regions of the finline cavity are given by

$$E_x^{(1)} = \sum_{n=1}^{\infty}\sum_{m=1}^{\infty} A_{mn1}\cos\left[\Gamma_{mn1}(x-h_1)\right] \cdot \sin(\alpha_n y)\sin(\beta_m z) \tag{1a}$$

$$H_x^{(1)} = \sum_{n=0}^{\infty}\sum_{m=0}^{\infty} B_{mn1}\sin\left[\Gamma_{mn1}(x-h_1)\right] \cdot \cos(\alpha_n y)\cos(\beta_m z) \tag{1b}$$

$$E_x^{(2)} = \sum_{n=1}^{\infty}\sum_{m=1}^{\infty} \left[A_{mn2}\sin(\Gamma_{mn2}x) + A'_{mn2}\cos(\Gamma_{mn2}x)\right] \cdot \sin(\alpha_n y)\sin(\beta_m z) \tag{1c}$$

$$H_x^{(2)} = \sum_{n=0}^{\infty}\sum_{m=0}^{\infty} \left[B_{mn2}\cos(\Gamma_{mn2}x) + B'_{mn2}\sin(\Gamma_{mn2}x)\right] \cdot \cos(\alpha_n y)\cos(\beta_m z) \tag{1d}$$

$$E_x^{(3)} = \sum_{n=1}^{\infty}\sum_{m=1}^{\infty} A_{mn3}\cos\left[\Gamma_{mn1}(x+d+h_2)\right] \cdot \sin(\alpha_n y)\sin(\beta_m z) \tag{1e}$$

$$H_x^{(3)} = \sum_{n=0}^{\infty}\sum_{m=0}^{\infty} B_{mn3}\sin\left[\Gamma_{mn1}(x+d+h_2)\right] \cdot \cos(\alpha_n y)\cos(\beta_m z) \tag{1f}$$

$$\Gamma_{mn1} = \sqrt{k_0^2 - \alpha_n^2 - \beta_m^2} \tag{2a}$$

$$\Gamma_{mn2} = \sqrt{k_0^2\epsilon_r - \alpha_n^2 - \beta_m^2} \tag{2b}$$

$$\alpha_n = \frac{2n\pi}{b} \tag{2c}$$

$$k_0 = \omega\sqrt{\mu_0\epsilon_0} \tag{2d}$$

and

$$\beta_m = \frac{m\pi}{(l+s)} \quad \text{for electric wall at } PP' \tag{2e}$$

$$= \left(\frac{2m+1}{2}\right)\cdot\frac{\pi}{(l+s)} \quad \text{for magnetic wall at } PP'. \tag{2f}$$

The field equations given by (1) satisfy the boundary conditions at the four boundary walls of the waveguide.

Manuscript received August 12, 1987; revised April 8, 1988.

The authors are with the Centre for Applied Research in Electronics, Indian Institute of Technology, Hauz Khas, New Delhi 110 016, India.

IEEE Log Number 8822042.

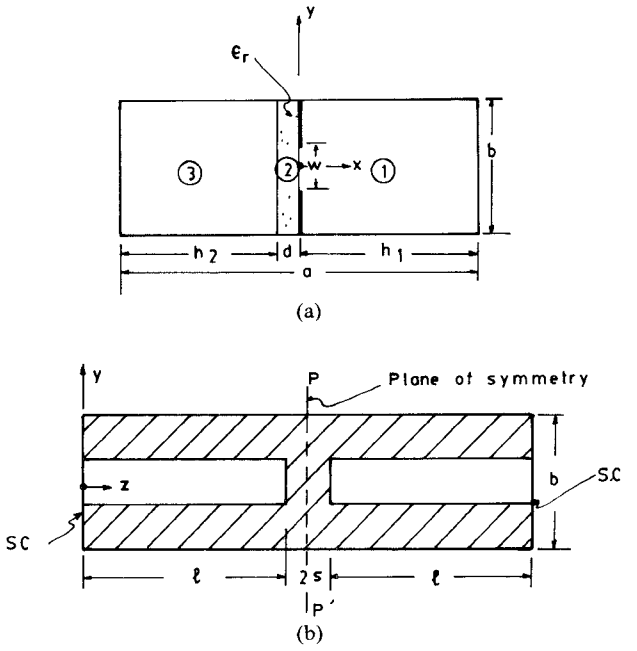

Fig. 1. (a) Cross-sectional view of unilateral finline. (b) Pattern on the substrate.

The y and z components of the electric and magnetic fields can be derived easily by using (1) in Maxwell's equations. Next, by applying the boundary conditions at $x = 0$ and $x = -d$, we obtain

$$A_{mn2} = \frac{\Gamma_{mn1}}{\Gamma_{mn2}} \cdot A_{mn1} \sin(\Gamma_{mn1} h_1) \tag{3a}$$

$$B_{mn2} = -B_{mn1} \sin(\Gamma_{mn1} h_1) \tag{3b}$$

$$A'_{mn2} = A_{mn2} F_1 \tag{3c}$$

$$B'_{mn2} = B_{mn2} F_2 \tag{3d}$$

where

$$F_1 = \frac{\epsilon_r \Gamma_{mn1} \sin(\Gamma_{mn2} d) \sin(\Gamma_{mn1} h_2) - \Gamma_{mn2} \cos(\Gamma_{mn2} d) \cos(\Gamma_{mn1} h_2)}{\epsilon_r \Gamma_{mn1} \cos(\Gamma_{mn2} d) \sin(\Gamma_{mn1} h_2) + \Gamma_{mn2} \sin(\Gamma_{mn2} d) \cos(\Gamma_{mn1} h_2)} \tag{4a}$$

$$F_2 = \frac{\Gamma_{mn1} \cos(\Gamma_{mn2} d) \cos(\Gamma_{mn1} h_2) - \Gamma_{mn2} \sin(\Gamma_{mn2} d) \sin(\Gamma_{mn1} h_2)}{\Gamma_{mn1} \sin(\Gamma_{mn2} d) \cos(\Gamma_{mn1} h_2) + \Gamma_{mn2} \cos(\Gamma_{mn2} d) \sin(\Gamma_{mn1} h_2)}. \tag{4b}$$

The slot field components at $x = 0$ are obtained as

$$E_y(y,z) = -\sum_{n=0}^{\infty} \sum_{m=1}^{\infty} S_{mn1} \cdot \sin(\Gamma_{mn1} h_1) \cos(\alpha_n y) \sin(\beta_m z) \tag{5a}$$

$$E_z(y,z) = -\sum_{n=1}^{\infty} \sum_{m=0}^{\infty} C_{mn1} \cdot \sin(\Gamma_{mn1} h_1) \sin(\alpha_n y) \cos(\beta_m z) \tag{5b}$$

where

$$S_{mn1} = \frac{1}{(\alpha_n^2 + \beta_m^2)} [-\Gamma_{mn1} \alpha_n A_{mn1} + j\omega\mu_0 \beta_m B_{mn1}] \tag{6a}$$

$$C_{mn1} = \frac{1}{(\alpha_n^2 + \beta_m^2)} [-\Gamma_{mn1} \beta_m A_{mn1} - j\omega\mu_0 \alpha_n B_{mn1}]. \tag{6b}$$

By applying the orthogonality condition to (5), the field coefficients A_{mn1} and B_{mn1} can be expressed in terms of the slot field distributions. The expressions are

$$A_{mn1} = \frac{1}{b(l+s)} \cdot \frac{\alpha_n P_n Q_m L_{1mn} + \beta_m P_m Q_n L_{2mn}}{\Gamma_{mn1} \sin(\Gamma_{mn1} h_1)} \tag{7a}$$

and

$$B_{mn1} = \frac{1}{b(l+s)} \cdot \frac{\alpha_n P_m Q_n L_{2mn} - \beta_m P_n Q_m L_{1mn}}{j\omega\mu_0 \sin(\Gamma_{mn1} h_1)} \tag{7b}$$

where

$$P_{n,m} = 1 \quad \text{for } n, m = 0 \tag{7c}$$
$$= 2 \quad \text{otherwise}$$

$$Q_{n,m} = 0 \quad \text{for } n, m = 0 \tag{7d}$$
$$= 2 \quad \text{otherwise.}$$

L_{1mn} and L_{2mn} are the transformed field components, which are expressed in terms of the slot field distributions as

$$L_{1mn} = \int_0^{l+s} \int_{-b/2}^{b/2} E_y(y,z) \cos(\alpha_n y) \sin(\beta_m z)\, dy\, dz \tag{8a}$$

$$L_{2mn} = \int_0^{l+s} \int_{-b/2}^{b/2} E_z(y,z) \sin(\alpha_n y) \cos(\beta_m z)\, dy\, dz. \tag{8b}$$

Next, by applying the boundary condition, namely $-(\vec{H}_{\tan}^{(1)} - \vec{H}_{\tan}^{(2)}) X\hat{x} = \vec{I}$ at $x = 0$, we obtain the following coupled algebraic equations in terms of the transformed fields:

$$\sum_{n=0}^{\infty} \sum_{m=1}^{\infty} P_n Q_m G_{11} L_{1mn} \sin(\beta_m z) \cos(\alpha_n y) + \sum_{n=0}^{\infty} \sum_{m=1}^{\infty} P_m Q_n G_{12} L_{2mn} \sin(\beta_m z) \cos(\alpha_n y) = b \cdot (l+s) \cdot I_y(y,z) \tag{9a}$$

$$\sum_{n=1}^{\infty} \sum_{m=0}^{\infty} P_n Q_m G_{21} L_{1mn} \sin(\alpha_n y) \cos(\beta_m z) + \sum_{n=1}^{\infty} \sum_{m=0}^{\infty} P_m Q_n G_{22} L_{2mn} \sin(\alpha_n y) \cos(\beta_m z) = b \cdot (l+s) \cdot I_z(y,z) \tag{9b}$$

where

$$G_{11}=\frac{\frac{j\omega\epsilon_0\alpha_n^2}{\Gamma_{mn1}}\left[\cos(\Gamma_{mn1}h_1)-\epsilon_r F_1\frac{\Gamma_{mn1}}{\Gamma_{mn2}}\sin(\Gamma_{mn1}h_1)\right]-\frac{\beta_m^2}{j\omega\mu_0}\left[\Gamma_{mn1}\cos(\Gamma_{mn1}h_1)+\Gamma_{mn2}F_2\sin(\Gamma_{mn1}h_1)\right]}{(\alpha_n^2+\beta_m^2)\sin(\Gamma_{mn1}h_1)} \tag{10a}$$

$$G_{12}=\frac{\frac{j\omega\epsilon_0\alpha_n\beta_m}{\Gamma_{mn1}}\left[\cos(\Gamma_{mn1}h_1)-\epsilon_r F_1\frac{\Gamma_{mn1}}{\Gamma_{mn2}}\sin(\Gamma_{mn1}h_1)\right]+\frac{\alpha_n\beta_m}{j\omega\mu_0}\left[\Gamma_{mn1}\cos(\Gamma_{mn1}h_1)+\Gamma_{mn2}F_2\sin(\Gamma_{mn1}h_1)\right]}{(\alpha_n^2+\beta_m^2)\sin(\Gamma_{mn1}h_1)} \tag{10b}$$

$$G_{21}=G_{12} \tag{10c}$$

$$G_{22}=\frac{\frac{j\omega\epsilon_0\beta_m^2}{\Gamma_{mn1}}\left[\cos(\Gamma_{mn1}h_1)-\epsilon_r F_1\frac{\Gamma_{mn1}}{\Gamma_{mn2}}\sin(\Gamma_{mn1}h_1)\right]-\frac{\alpha_n^2}{j\omega\mu_0}\left[\Gamma_{mn1}\cos(\Gamma_{mn1}h_1)+\Gamma_{mn2}F_2\sin(\Gamma_{mn1}h_1)\right]}{(\alpha_n^2+\beta_m^2)\sin(\Gamma_{mn1}h_1)}. \tag{10d}$$

In (9), $I_y(y,z)$ and $I_z(y,z)$ represent the y and z components of the current density on the fins.

We now express L_{1mn} and L_{2mn} in terms of series of the form

$$L_{1mn}=\sum_{p=0}^{\infty}\sum_{q=0}^{\infty}c_{pq}L_{1mn}^{(p,q)} \tag{11a}$$

$$L_{2mn}=\sum_{p=0}^{\infty}\sum_{q=0}^{\infty}d_{pq}L_{2mn}^{(p,q)}. \tag{11b}$$

Next, application of the Ritz–Galerkin method followed by the use of Parseval's theorem in transformed domain enables us to eliminate the fin current components I_y and I_z from (9). We then obtain a linear system of homogeneous equations given by

$$\sum_{p=0}^{\infty}\sum_{q=0}^{\infty}c_{pq}\sum_{n=0}^{\infty}\sum_{m=1}^{\infty}P_nQ_mG_{11}L_{1mn}^{(p,q)}L_{1mn}^{(i,j)} + \sum_{p=0}^{\infty}\sum_{q=0}^{\infty}d_{pq}\sum_{n=0}^{\infty}\sum_{m=1}^{\infty}P_mQ_nG_{12}L_{2mn}^{(p,q)}L_{1mn}^{(i,j)}=0 \tag{12a}$$

$$\sum_{p=0}^{\infty}\sum_{q=0}^{\infty}c_{pq}\sum_{n=1}^{\infty}\sum_{m=0}^{\infty}P_nQ_mG_{21}L_{1mn}^{(p,q)}L_{2mn}^{(i,j)} + \sum_{p=0}^{\infty}\sum_{q=0}^{\infty}d_{pq}\sum_{n=1}^{\infty}\sum_{m=0}^{\infty}P_mQ_nG_{22}L_{2mn}^{(p,q)}L_{2mn}^{(i,j)}=0, \quad i=0,1,2,\cdots,\infty \quad j=0,1,2,\cdots,\infty. \tag{12b}$$

For a specific frequency, the dominant mode resonant length l_e for the odd mode and l_m for the even mode of the cavity can be obtained by equating the determinant of the coefficient matrix to zero for each of the two cases separately.

From the equivalent circuit for the even- and odd-mode cases given in Fig. 2, the resonant condition for the cavity in terms of the normalized impedance parameters of a symmetric discontinuity is given by

$$\bar{X}_{se}+j\tan(\beta l_e)=0 \tag{13a}$$

and

$$\bar{X}_{se}+2\bar{X}_{sh}+j\tan(\beta l_m)=0. \tag{13b}$$

It is assumed that only the dominant mode propagates in the finline section. In (13), β is the phase constant for the dominant mode in finline. $\bar{X}_{se}$ $(=X_{se}/Z_0)$ and $\bar{X}_{sh}$ $(=X_{sh}/Z_0)$ are the normalized series and shunt impedance parameters, respectively, of the equivalent T network of the discontinuity, and Z_0 is the characteristic impedance of the finline of slot width w.

III. Slot Field Distribution

The choice of the slot field distribution in the presence of a discontinuity is rather critical for the evaluation of the resonator lengths l_e and l_m. In order to take into account the end effect due to the presence of the strip discontinuity, the z-dependent basis function is chosen as a modified sine distribution for the E_y component and a modified cosine distribution for the E_z component. These distributions are illustrated in Fig. 3. The y and z components of the slot field distribution are expressed as

$$E_y(y,z)=cf_1(y)\cdot f_1(z) \tag{14a}$$

$$E_z(y,z)=df_2(y)\cdot f_2(z) \tag{14b}$$

where

$$f_1(y)=\left[(w/2)^2-y^2\right]^{-1/2}, \qquad |y|\leq w/2 \tag{15a}$$

$$f_2(y)=y\cdot\left[(w/2)^2-y^2\right]^{1/2}, \qquad |y|\leq w/2 \tag{15b}$$

$$f_1(z)=\sin\left(\frac{2\pi z}{\lambda'}\right), \qquad 0<z\leq\lambda'/4$$
$$=\sin\left[\frac{\pi(l_{e,m}-z)}{2l_{e,m}-\lambda'/2}\right], \qquad \lambda'/4<z\leq l_{e,m} \tag{15c}$$

$$f_2(z)=\cos\left(\frac{2\pi z}{\lambda'}\right), \qquad 0<z\leq\lambda'/4$$
$$=-\cos\left[\frac{\pi(l_{e,m}-z)}{2l_{e,m}-\lambda'/2}\right], \qquad \lambda'/4<z\leq l_{e,m}. \tag{15d}$$

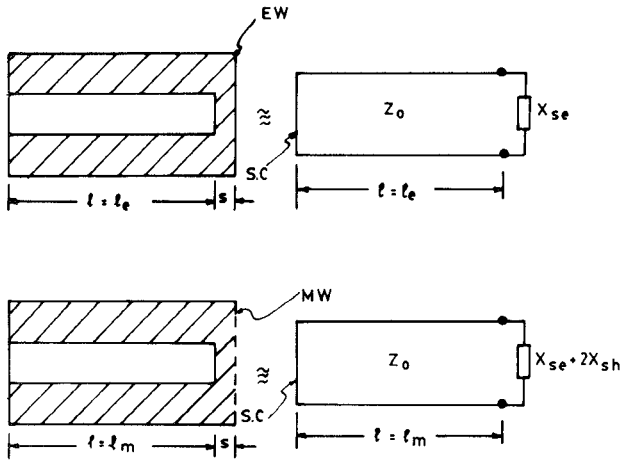

Fig. 2. Equivalent circuit of a symmetrical inductive strip in finline cavity for (a) odd mode and (b) even mode excitations.

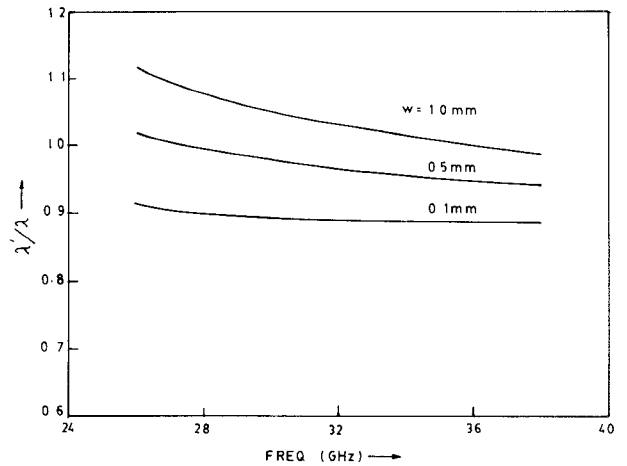

Fig. 4. Dispersion characteristic of a unilateral finline: waveguide = WR(28), $\epsilon_r = 2.22$, $d = 0.254$ mm, and $h_1 = 3.556$ mm

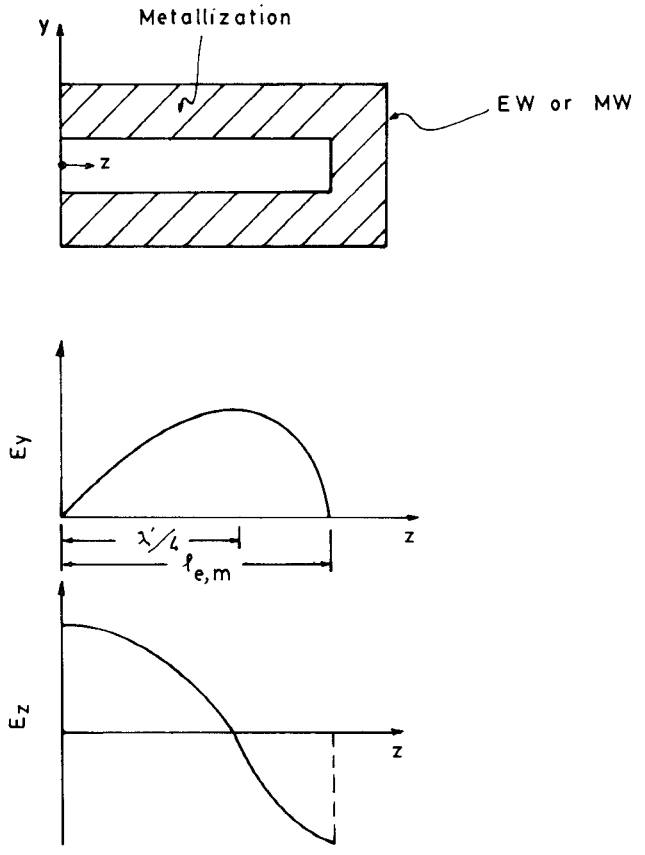

Fig. 3. z-dependent slot field distributions in finline cavity.

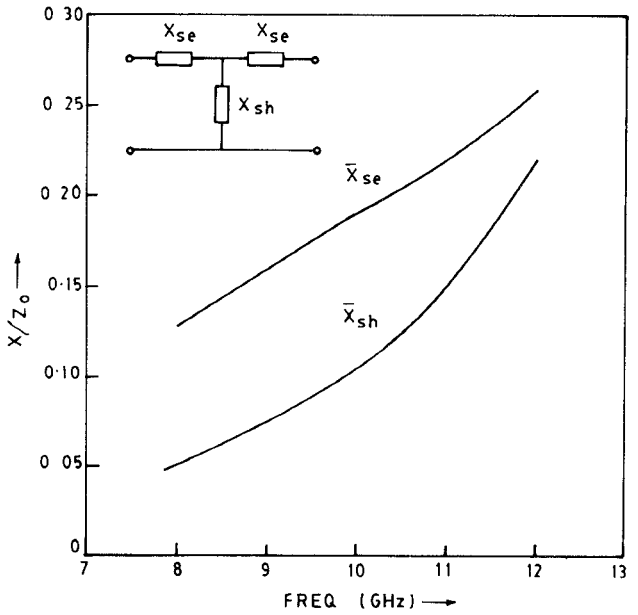

Fig. 5. Equivalent circuit parameters of an inductive strip in unilateral finline: waveguide = WR(90), $2s = 0.508$ mm, $\epsilon_r = 1.0$, $w/b = 0.25$, and $h_1 = 11.43$ mm.

Here c and d are unknown coefficients and λ' is the guide wavelength of the dominant mode in finline.

It may be noted that as the septum width reduces to zero, the z-dependent slot field distribution reduces to a sinusoid.

IV. Results

We first compute the guide wavelength λ' in finline by considering the formulas for the odd-mode excitation and setting the strip width equal to zero. The lowest resonant length for a given frequency will then be equal to half the wavelength in the finline. Fig. 4 shows the plot of the normalized guide wavelength λ'/λ (where λ is the free-space wavelength) with frequency for different slot widths. These computations were carried out by taking 50 terms and also 100 terms in the series expansion of (12), and the difference in the two results of λ'/λ was less than 0.5 percent.

Fig. 5 shows the plot of the computed values of equivalent impedance parameters of an inductive strip as a function of frequency at X-band. As the frequency increases, the normalized shunt reactance $\bar{X}_{sh}$ increases almost exponentially. This indicates that the coupling between two resonator sections is due to higher order evanescent modes. In Fig. 6, the computed data on the magnitude and phase of the reflection coefficient of the inductive strip are compared with the theoretical and experimental results reported by Knorr and Deal [3]. The

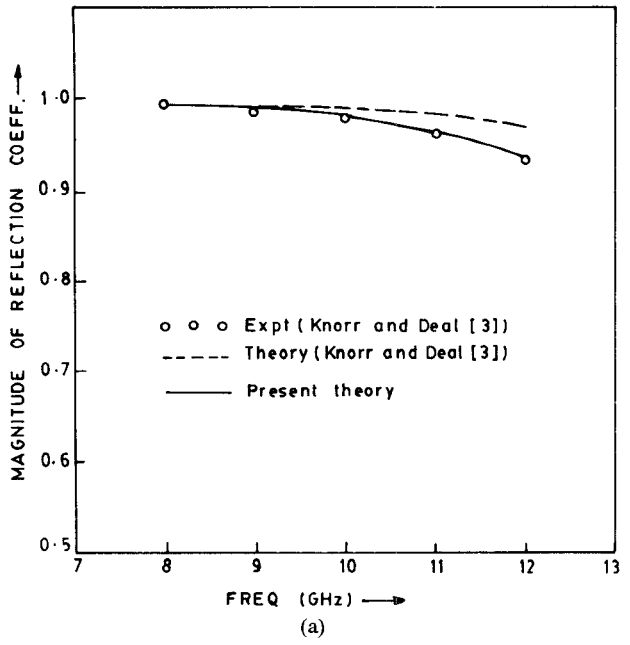

Fig. 6. Comparison of (a) magnitude and (b) phase of reflection coefficient of an inductive strip in unilateral finline with the results of Knorr and Deal [3]. Waveguide = WR(90), $\epsilon_r = 1.0$, $2s = 0.508$ mm, $w/b = 0.25$, and $h_1 = 11.43$ mm.

present theoretical results are better than those of Knorr and Deal [3], mainly due the improved basis function chosen for the z-dependent field distribution for the E_y component. Computations showed that inclusion of the E_z component in the slot field distribution has a negligible effect on the results of resonant lengths. For example, the numerical results of l_e and l_m (expressed in mm) computed with and without the E_z component were found to match up to the second decimal place.

Fig. 7 shows a comparison of theoretical and experimental results of the transmission coefficient of an inductive

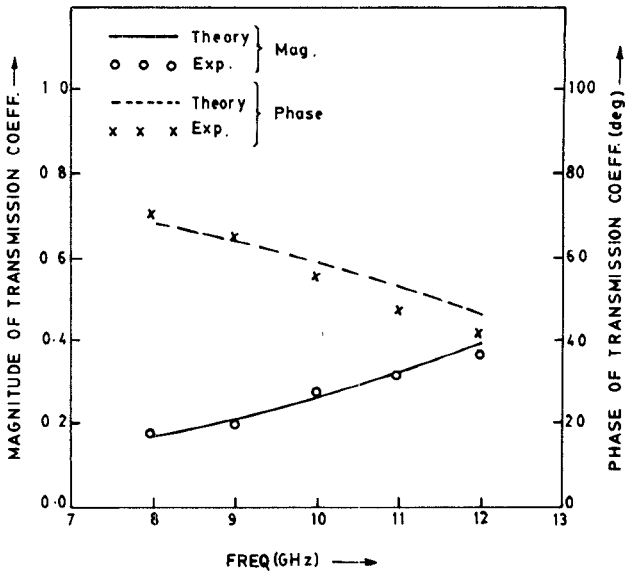

Fig. 7. Comparison of theoretical and experimental results of the transmission coefficient of an inductive strip in unilateral finline: waveguide = WR (90), $\epsilon_r = 2.22$, $2s = 2.90$ mm, $w = 2.13$ mm, and $h_1 = 11.43$ mm.

strip in finline with RT-duroid as dielectric substrate. For experimental measurement, two finline sections of fixed length, one with the inductive strip and other without, were considered. The magnitude of the transmission coefficient was obtained from the difference in the transmission loss between the two finline sections as measured on the network analyzer. The phase of the transmission coefficient was determined by subtracting the insertion phase of the two sections and incorporating a correction due to the physical length of the inductive strip.

V. Conclusions

The modeling of inductive strip discontinuity in finline has been carried out using the hybrid-mode analysis in conjunction with the transverse resonance technique. It is shown that an appropriate modification in the commonly assumed sinusoidal distribution for the z-dependent basis function allows an accurate characterization of the strip discontinuity.

References

[1] A. M. K. Saad and K. Schunemann, "A rectangular waveguide equivalent for bilateral and unilateral finline," *Arch. Elek. Übertragung.*, vol. 35, no. 7, pp. 287–292, 1981.

[2] N. H. L. Koster and R. H. Jansen, "Some new results on the equivalent circuit parameters of the inductive strip discontinuity in unilateral finline," *Arch. Elek. Übertragung.*, vol. 35, no. 12, pp. 497–499, 1981.

[3] J. B. Knorr and J. C. Deal, "Scattering coefficient of an inductive strip in a finline: Theory and experiment," *IEEE Trans. Microwave Theory Tech.*, vol. MTT-33, Oct. 1985.

[4] H. El Hennawy and K. Schunemann, "Impedance transformation in finline," *Proc. Inst. Elec. Eng.*, pt. H, vol. 129, pp. 342–350, Dec. 1982.

[5] R. Sorrentino and T. Itoh, "Transverse resonance analysis of finline discontinuities," *IEEE Trans. Microwave Theory Tech.*, vol. MTT-32, pp. 1633–1638, Dec. 1984.

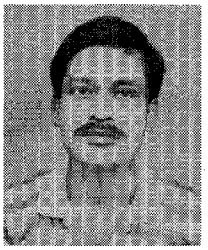

Animesh Biswas (S'85) was born in West Bengal, India. He received the B.E. degree in electronics and telecommunication from Calcutta University, India, in 1980 and the M. Tech degree from the Indian Institute of Technology, Kharagpur, India, in 1982.

Since 1982, he has been working as Assistant Executive Engineer with Indian Telephone Industries Ltd., (I.T.I.), Bangalore. From July 1984 to December 1988, he was on leave from I.T.I. to pursue the Ph.D. degree at the Indian Institute of Technology, New Delhi. His main areas of interest are the analysis and design of microwave and millimeter-wave integrated circuits.

✠

Bharathi Bhat (SM'82) received the B.E. and M.E. degrees (both with distinction) from the Indian Institute of Science, Bangalore, India, in 1963 and 1965, respectively, and the M.S. and Ph.D. degrees from the Division of Engineering and Applied Physics, Harvard University, Cambridge, MA, in 1967 and 1971, respectively.

From 1971 to 1972, she worked as a postdoctoral research fellow at Harvard University. In 1973, she joined the Indian Institute of Technology, New Delhi, as Assistant Professor. Since 1977, she has been a Professor at the Centre for Applied Research in Electronic (C.A.R.E.), I.I.T., Delhi. She is presently the head of C.A.R.E. She is also the leader of the Microwave Group and has been directing a number of sponsored research projects in the areas of microwave antennas, electronic phase shifters, and microwave and millimeter-wave integrated circuits and components.

Dr. Bhat is the recipient of the Ram Lal Wadhwa Gold Medal (1983), and the Shri Hari Om Prerit Dr. Vikram Sarabhai Research Award (1985) for her outstanding contributions in the field of electronics and telecommunications in India. She is a Fellow of the Institute of Electronics and Telecommunication Engineers (IETE) and of the Indian National Academy of Engineers (INAE), India. She has served as the Honorary Editor of the *IETE Journal* (1981–82), member of the IETE Council (1982–84), and Chairman of ED/MTT Chapter of the IEEE India Council (1983–84). Presently, she is a member of the IETE Council, the INAE Council, and Commission B of the Indian National Committee of URSI.